A Normative Data Set for the Clinical Assessment of Achromatic and Chromatic Contrast Sensitivity Using a *qCSF* Approach

Yeon Jin Kim, Alexandre Reynaud, Robert F. Hess, and Kathy T. Mullen

McGill Vision Research, Department of Ophthalmology, McGill University, Montreal, Quebec, Canada

Correspondence: Kathy T. Mullen, McGill Vision Research, Department of Ophthalmology, McGill University, Room L11.513, 1650 Cedar Avenue, Montreal, Quebec H3G 1A4, Canada; kathy.mullen@mcgill.ca.

Submitted: February 8, 2017
Accepted: June 19, 2017

Citation: Kim YJ, Reynaud A, Hess RF, Mullen KT. A normative data set for the clinical assessment of achromatic and chromatic contrast sensitivity using a *qCSF* approach. *Invest Ophthalmol Vis Sci*. 2017;58:3628–3636. DOI:10.1167/iovs.17-21645

Purpose. The measurement of achromatic sensitivity has been an important tool for monitoring subtle changes in vision as the result of disease or response to therapy. In this study, we aimed to provide a normative data set for achromatic and chromatic contrast sensitivity functions within a common cone contrast space using an abbreviated measurement approach suitable for clinical practice. In addition, we aimed to provide comparisons of achromatic and chromatic binocular summation across spatial frequency.

Methods. We estimated monocular cone contrast sensitivity functions (CCSFs) using a quick Contrast Sensitivity Function (qCSF) approach for achromatic as well as isoluminant, L/M cone opponent, and S cone opponent stimuli in a healthy population of 51 subjects. We determined the binocular CCSFs for achromatic and chromatic vision to evaluate the degree of binocular summation across spatial frequency for these three different mechanisms in a subset of 20 subjects.

Results. Each data set shows consistent contrast sensitivity across the population. They highlight the extremely high cone contrast sensitivity of L/M cone opponency compared with the S-cone and achromatic responses. We also find that the two chromatic sensitivities are correlated across the healthy population. In addition, binocular summation for all mechanisms depends strongly on stimulus spatial frequency.

Conclusions. This study, using an approach well suited to the clinic, is the first to provide a comparative normative data set for the chromatic and achromatic contrast sensitivity functions, yielding quantitative comparisons of achromatic, L/M cone opponent, and S cone opponent chromatic sensitivities as a function of spatial frequency.

Keywords: color vision, isoluminance, cone contrast sensitivity, contrast sensitivity function

Ever since it was first introduced into clinical practice by Gstalder and Green[1] more than 40 years ago, the measurement of achromatic contrast sensitivity has been an important tool for monitoring subtle changes in vision as the result of disease or in response to therapy.[2–7] However, a comprehensive assessment of visual function should go beyond the measurement of achromatic contrast sensitivity, based on the summing of cone outputs, and also include chromatic sensitivity, derived from the two postreceptoral, cone-opponent processes. One process, loosely termed red-green (RG), is L/M cone opponent and is associated with the midget bipolar and midget ganglion cells of the primate retina and the P cell layers of the lateral geniculate nucleus (LGN). The other, loosely termed blue-yellow (BY), opposes the S cones against the combined L and M cones, using distinct retinal cells (i.e., S-cone bipolar, small bistratified, large sparse monostratified, and large sparse bistratified ganglion cells)[8–10] that project to the K cell layers of the LGN.[11] A comparison of the sensitivities of all three mechanisms requires a common stimulus metric that allows both chromatic and achromatic stimuli to be represented using the same physical units, and this is typically cone contrast. Within the three-dimensional cone contrast space, stimulus chromaticity is represented by the proportional modulations of the three cone types (vector direction) and cone contrast by the magnitude of the cone modulations (vector length).[12–14] Hence, measurements of detection thresholds for different chromatic and achromatic stimuli yield their respective cone contrast sensitivities (CCSs) within this common biological metric, allowing them to be directly compared.

It is well known that there are characteristic differences between the chromatic and achromatic responses in terms of the shapes of the spatial contrast sensitivity functions (CSF). The chromatic CSF is spatially lowpass with optimal contrast sensitivity at spatial frequencies below 0.5 cycles/degree (c/d), in comparison to the bandpass, high-acuity form of the achromatic CSF.[15,16] The combined measurement of achromatic and chromatic contrast sensitivity across spatial frequency provides a comprehensive assessment of visual function from retina to cortex and ideally should be incorporated into clinical practice. There have been no direct comparisons of the three spatial CCS functions for the RG, BY, and achromatic postreceptoral mechanisms, although this has been done for temporal frequency in a limited number of subjects.[17] There is also no normative data base for both achromatic and chromatic CCSs as a basis for assessing an individual patient's results, although the study by Rabin et al.[18] compared in a large population the detection thresholds of letters along the three

individual cone axes within a cone contrast space, as a successful test of inherited color vison deficiencies. A further obstacle is that traditionally the measurement of these sensitivities in the laboratory has required time-consuming psychophysical procedures that are not well suited to the clinic.

In the present study, we sought to overcome these obstacles with the aim of facilitating the use of contrast sensitivity in all of its forms in the clinic. We provide a normative data set ($n = 51$) for achromatic as well as chromatic (RG and BY) CCS functions (CCSFs) measured with the quick Contrast Sensitivity Function (*qCSF*) approach.[19,20] Further, we characterized the binocular CCSFs for achromatic and chromatic vision in a subset of 20 young adults to derive the degree of binocular summation (binocular/monocular sensitivity) as a function of spatial frequency for these three different systems. In addition to providing this normative data set, we reveal two interesting findings. First, the two chromatic (RG versus BY) sensitivities exhibit correlations across the healthy population. Second, binocular summation for all mechanisms depends strongly on stimulus spatial frequency.

Methods

Apparatus

Stimuli were generated using a ViSaGe videographic card (Cambridge Research Systems, Kent, UK) with 14-bit contrast resolution and presented on a Sony Trinitron (GDM 500DIS) monitor (Sony Corporation, Tokyo, Japan) at 120-Hz frame rate and 1024 × 768 spatial resolution. The monitor was gamma corrected using the VSG calibration routine with the OptiCal photometer (Cambridge Research Systems). The spectral emission functions of the red, green, and blue phosphors of the monitor were measured using a Spectra Scan PR-645 spectrophotometer (Photo Research, Inc., Chatsworth, CA, USA). The CIE-1931 chromaticity coordinates of the red, green, and blue phosphors were ($x = 0.610$, $y = 0.333$), ($x = 0.302$, $y = 0.591$), and ($x = 0.153$, $y = 0.084$), respectively. The background was achromatic, with a mean luminance of 51 cd/m^2 at the screen center. Stimuli were viewed at a distance of 58 cm in a dimly lit room, with a patch on the nondominant eye (self-reported) for the monocular condition and without it for the binocular condition. Chromatic and achromatic stimuli were controlled independently by lookup tables.

Observers

Fifty-one subjects between 19 and 59 years (mean age 25.8 ± 7.2 SD, 25 females, 26 males), including three authors and 48 naïve subjects, participated in the main experiment. Twenty participated in the binocular experiment and six participated in the control experiment. All subjects had normal or corrected-to-normal visual acuity, and normal stereopsis tested with the three-book Randot Preschool Stereoacuity Test (Stereo Optical Co., Inc., Chicago, IL, USA).[21] Participants were screened for normal color vision using the Farnsworth/Lanthony Combined D-15 Test (Gulden Ophthalmics, Elkins Park, PA, USA). The experiments were performed in accordance with the Declaration of Helsinki and approved by the institutional ethics committee of McGill University Health Center. Each subject signed an informed consent form.

Stimuli and Color Space

Stimuli consisted of either horizontal- or vertical-oriented bandpass filtered noise generated in the space domain by filtering white noise by a Gabor filter with a spatial frequency bandwidth of 1.84 octaves and were presented in a Gaussian window with a sigma of 5° (Fig. 1a). This is essentially a stimulus with the same amplitude spectrum as a windowed grating but with a more complex phase spectrum. One advantage is that any normative data can be more easily related to future studies using second-order modulations that use a bandpass noise carrier. Another possible advantage is that the areas of peak and trough stimulation (e.g., red versus green, blue versus yellow) are varied on a trial-by-trial basis. Stimulus peak spatial frequency and contrast were varied. Stimuli were presented for 1 second with an abrupt onset/offset.

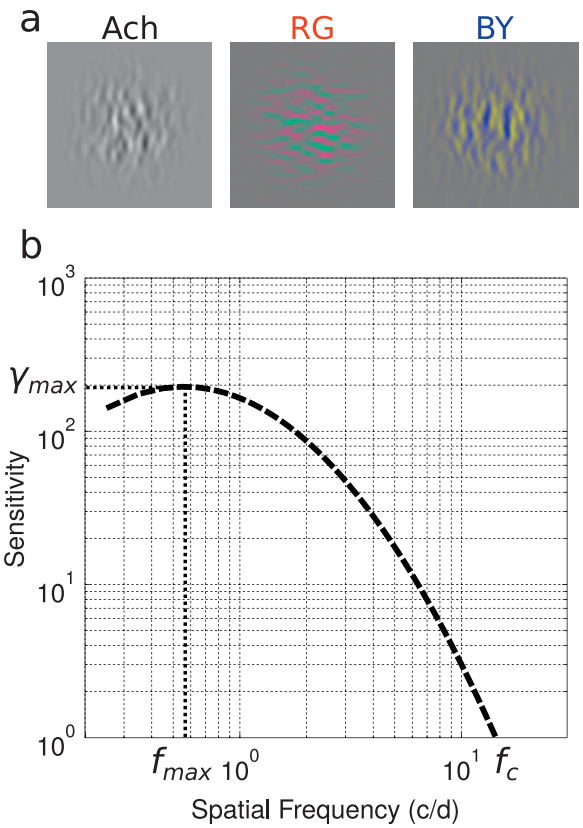

Figure 1. (**a**) Three examples of the stimuli: oriented (either vertical or horizontal) filtered noise patterns for the Ach (*left*), the RG (*middle*), and the BY (*right*) cone contrasts, each isolating the L+M (often referred to as the luminance mechanism), L-M (referred to as the RG mechanism), S-(L+M) (referred to as the BY mechanism) mechanisms, respectively. (**b**) An example of CCS across spatial frequency estimated by the *qCSF* method that assumes the sensitivity function has a log-parabola shape characterized by its peak gain γ_{max}, peak spatial frequency f_{max}, and cutoff spatial frequency f_c parameters.

The three types of stimuli used were cardinal, isolating the achromatic (Ach), RG, and BY postreceptoral processes, respectively (Fig. 1a). Stimuli were represented in a three-dimensional cone contrast space[13,14] in which each axis represents the response of the L-, M-, or S-cone type normalized to the response to the white background. Cone contrast was calculated using the cone fundamentals of Smith and Pokorny,[22] with a linear transform calculated to specify the required phosphor contrasts of the monitor for given cone contrasts. Stimulus contrast is defined as the vector length in cone contrast units (Cc):

$$C_C = \sqrt{(L_C)^2 + (M_C)^2 + (S_C)^2} \quad (1)$$

where L_C, M_C, and S_C represent the L, M, and S Weber cone contrast fractions in relation to the L-, M-, and S-cone values of the achromatic background.[23] This contrast metric is higher by a factor of $\sqrt{3}$ (1.73) from the conventional luminance Michelson contrast. Stimulus chromaticity is given by vector direction. The achromatic cardinal stimulus has an L-, M-, and S-cone response ratio of 1:1:1 respectively, the BY cardinal stimulus is the S-cone axis of the cone contrast space (cone response ratio of 0:0:1) and the RG cardinal stimulus has an isoluminant direction in the L/M cone contrast plane and was determined individually for each subject using a minimum flicker task. To determine RG isoluminance, the subject viewed a counterphasing horizontal grating (4 Hz, 0.375 c/d) in a Gaussian envelope ($\sigma = 2°$) and a method of adjustment was used to determine the L:M cone ratio at which a minimum in perceived counterphase flicker occurred based on the average of 10 repeated measurements. The average RG isoluminant point across all 51 subjects, expressed as the L:M isoluminant cone ratio was 1:–1.83 (± 1.30 SD) (see Supplementary Fig. S1).

Procedures and Analysis

The subjects' task was to identify the orientation of the pattern in a single-interval identification task by pressing a button box after the stimulus disappeared. Audio feedback was provided. The CSFs $S(f)$ (Equation 2) were determined using the *qCSF* method.[19,20] The frequency range of the test was truncated from 0.24 to 2.39 c/d for chromatic conditions and from 0.24 to 9.57 c/d for achromatic conditions. In the orientation identification task, the *qCSF* was estimated with 100 trials, which took approximately 8 minutes and was repeated twice. The method estimates the log-sensitivity function with a truncated log-parabola model,[24,25] which is described by four parameters: the peak gain γ_{max}, the peak spatial frequency f_{max}, the bandwidth β, and the truncation δ, given in Equation 2 (see Fig. 1b).

$$\begin{aligned} S(f) &= \log_{10}(\gamma_{max}) - \kappa\left(\frac{\log_{10}(f) - \log_{10}(f_{max})}{\frac{\beta'}{2}}\right)^2 \\ S(f) &= \log(\gamma_{max}) - \delta \\ &\quad \text{if } f < f_{max} \quad \text{and} \quad S'(f) < \log_{10}(\gamma_{max}) - \delta \\ S(f) &= S'(f) \qquad \text{else} \end{aligned} \quad (2)$$

with $\kappa = \log_{10}(2)$ and $\beta' = \log_{10}(2\beta)$.

The initial gain prior (γ_{max}) was set to 100 for the Ach and BY conditions and 1000 for the RG condition. The peak frequency prior was set to 2 c/d and the bandwidth prior was set to 3 octaves in all conditions. We discarded the truncation parameter from our analyses because it was often out of the range of our measurements. The cutoff spatial frequency f_c was calculated in function of the other parameters, as the frequency for which the log-sensitivity is minimal $S = 0$ (Equation 3), thus the bandwidth was not analyzed because it became redundant.

$$f_c = f_{max} \cdot 10^{\frac{\beta'}{2}} \sqrt{\frac{\log_{10}(\gamma_{max})}{\kappa}} \quad (3)$$

Results

Figure 2 shows monocular CCSFs for the Ach (solid black line), RG (solid red line), and BY (solid blue line) conditions averaged across the 51 subjects. Results from each individual subject are plotted in Figure 3. As can be seen in Figures 2 and 3, the overall shapes of the CCSFs for the RG and BY stimuli are lowpass, as previously reported,[16,17] whereas Ach functions are more bandpass, resembling achromatic CSFs previously reported for low temporal frequencies.[26] As can be seen from Figure 2, the CCS for BY and Ach at 1 c/d is roughly equal. Similar results have been reported previously (see Figs. 3a, 3b from Wuerger et al.[27]). Here, the bandpass shape of the achromatic condition has a peak spatial frequency f_{max} at 1.63 c/d (see average estimated values in the Table). In comparison, for both the RG and BY chromatic conditions, the two lowpass functions have peak spatial frequencies f_{max} at 0.58 c/d and 0.49 c/d for the RG and BY conditions, respectively.

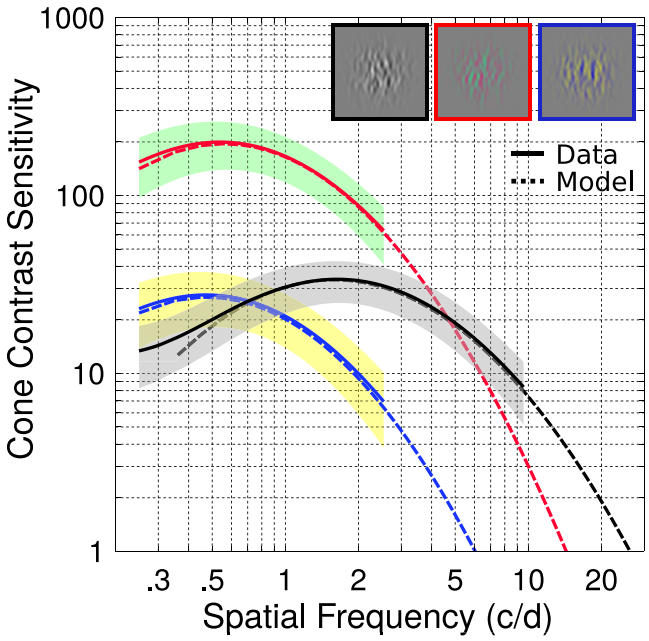

Figure 2. Measured CCS as a function of spatial frequency for the Ach (*solid black line*), RG (*solid red line*), and BY (*solid blue line*) conditions under monocular viewing. The average across the 51 subjects is shown. The *dotted lines* indicate the log-parabola model estimation, which is reconstructed with the average estimated values for each of the three parameters by the *qCSF*. The averaged model parameters are reported in the Table. The shaded regions represent ± SD.

The CCS for the RG chromatic condition is clearly greater than the other two. The estimated value of the peak gain γ_{max} for the RG condition averaged across the 51 subjects is 204.6, which is six and seven times higher than the Ach ($\gamma_{max} = 34.7$) and BY ($\gamma_{max} = 28.5$), respectively, which are similar to each other (see the Table). The superior CCS of the L/M cone opponent process compared with the other two mechanisms at low spatial frequencies is well known, particularly from the measurement of threshold contours in a cone contrast space.[13,14,28,29] We note that the advantage of using the cone contrast space is that it allows the two chromatic and the achromatic contrast sensitivities to be directly compared across a range of spatial frequencies.

The estimated values of the cutoff spatial frequency f_c for the achromatic condition averaged across the 51 subjects is 27.4 c/d, which is 1.9 and 4.4 times higher than the RG (14.8 c/d) and BY (6.3 c/d) ones, respectively (see the average estimated values in the Table). This result reflects the higher spatial resolution of the achromatic mechanism compared with the RG and BY chromatic mechanisms.[17,30]

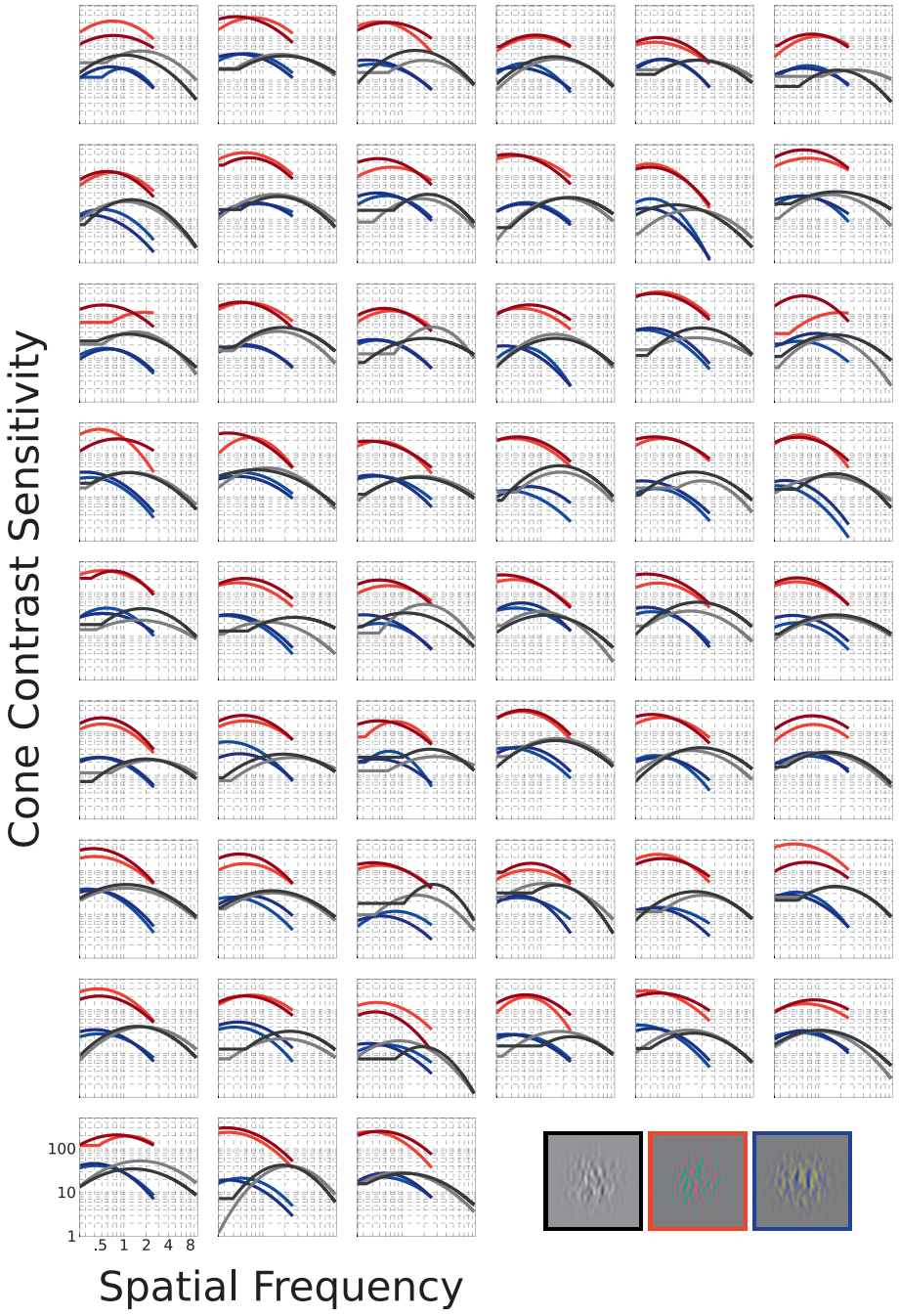

Figure 3. The individual CCSFs for the 51 subjects used to calculate the averages in Figure 2. Each panel indicates an individual's data in which each subject replicates two times for the Ach (*solid black line*), RG (*solid red line*), and BY (*solid blue line*) sensitivity measurements with the *qCSF*.

Table. Statistics of the Model Parameter Distributions for the Ach, RG, and BY Conditions Presented on the Right Side of Each Panel of Figure 4

	γmax			f_{max} (c/d)			f_c (c/d)		
Condition	μ	σ	c_v	μ	σ	c_v	μ	σ	c_v
Ach	34.68	8.71	0.25	1.63	0.39	0.24	27.42	8.41	0.31
RG	204.56	59.51	0.29	0.58	0.16	0.28	14.83	4.08	0.28
BY	28.46	9.46	0.33	0.49	0.12	0.24	6.26	1.72	0.28

Mean (μ), SD (σ), and coefficient of variation (c_v) of the distributions are presented for the peak gain γ_{max}, peak spatial frequency f_{max}, and cutoff spatial frequency f_c parameters.

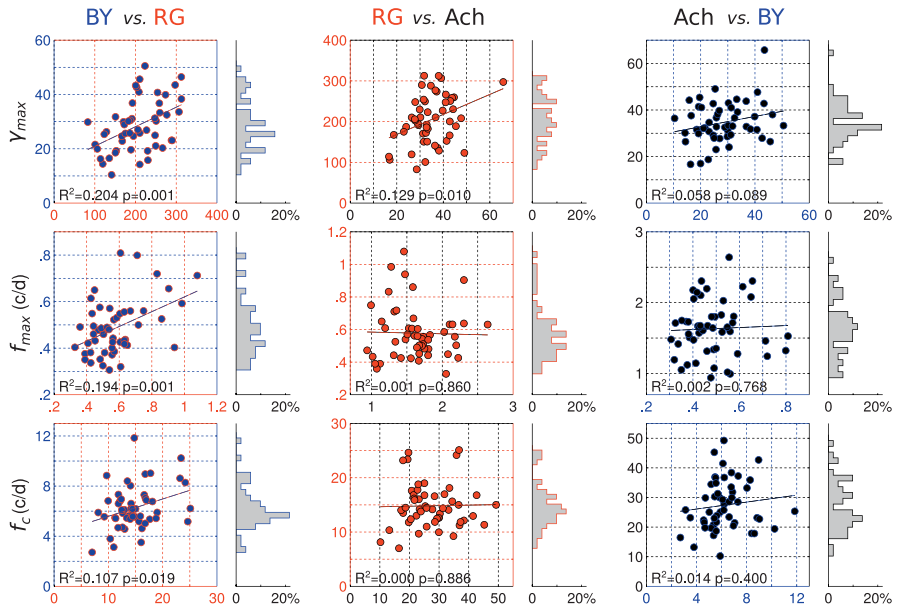

Figure 4. Parameter correlations. The estimated values for each of the peak gain γ_{max}, the peak spatial frequency f_{max}, and the cutoff spatial frequency f_c are correlated in the three pairs: (1) BY versus RG (*left column*); (2) RG versus Ach (*middle column*); and (3) Ach versus BY (*right column*). On the *right side* of each panel is plotted the distribution of the estimated values of the parameter represented in ordinates. Statistics of the model parameter distributions are given in the Table.

The distributions of the three model parameter estimates (γ_{max}, f_{max}, and f_c) across subjects for each of the achromatic, RG, and BY conditions are plotted in the right side of each panel in Figure 4. The average (μ), SD (σ), and coefficient of variation (c_v) of these distributions are given in the Table. The coefficient of variations in these parameters are approximately 0.3 for both the achromatic and chromatic (RG and BY) conditions. This finding indicates that mechanisms mediating the achromatic and chromatic sensitivities show the same variability. This variability is quite low, as can be seen in Figure 3. The CSFs of individual subjects are very reproducible over two measurements and consistent between subjects.

To further explore the relationship among the Ach, RG, and BY CSFs, we investigated the correlation between the tuning of their functions, represented by the peak gain γ_{max}, peak frequency f_{max}, and cutoff frequency f_c parameters. Figure 4 plots the correlation of each parameter (rows) in the three different pairs of comparisons (columns).

For the BY versus RG comparison (left column, Fig. 4), each of the three parameter estimates (γ_{max}, f_{max}, and f_c) are significantly correlated between the RG and BY conditions (γ_{max}: $R^2 = 0.204$, $P = 0.001$; f_{max}: $R^2 = 0.194$, $P = 0.001$; f_c: $R^2 = 0.107$, $P = 0.019$). Interestingly, this finding reveals a potential dependency between the RG and BY cone-opponent mechanisms.

For the RG versus Ach comparison (middle column, Fig. 4), the peak gain parameter γ_{max} only reveals a potential correlation between the RG and BY conditions (γ_{max}: $R^2 = 0.129$, $P = 0.010$). However, this effect is mainly due to one outlier subject with a very high achromatic sensitivity (S34, in the top right of the panel, see individual data in Fig. 3). Without this outlier, the coefficient of correlation R^2 for the peak gain between the RG and Ach conditions drops to 0.086 ($P = 0.039$). In comparison, the other two parameters show no significant correlation between the conditions (f_{max}: $R^2 = 0.001$, $P = 0.860$; f_c: $R^2 = 0.000$, $P = 0.886$).

For the Ach versus BY comparison (right column, Fig. 4), each of the three parameters reveals no correlation between the conditions (γ_{max}: $R^2 = 0.058$, $P = 0.089$; f_{max}: $R^2 = 0.002$, $P = 0.768$; f_c: $R^2 = 0.014$, $P = 0.400$). In addition, without the outlier subject (S34, in the top right of the panel) for the peak gain parameter, the coefficient of correlation R^2 between the Ach and BY conditions drops to 0.022 ($P = 0.303$).

In the next experiment, we evaluated binocular summation (the change in sensitivity when using two eyes as opposed to one) for a subset of 20 subjects. Figure 5a shows the measured monocular (solid line) and binocular (dotted line) CCSFs for the Ach, RG, and BY conditions (black, red, and blue lines, respectively), and Figure 5b plots the ratio of the binocular/monocular contrast sensitivities. Results show the binocular summation ratio declines with spatial frequency, with the two chromatic conditions showing a consistent decline and the Ach declining after 1 c/d. At the lowest spatial frequency (0.24 c/d), the ratio is approximately 1.8 for the achromatic and 1.9 for the BY conditions, and is approximately 2.1 for the RG condition. At the highest spatial frequency used for the two color conditions (2 c/d), the ratio drops to 1.5 for the RG and 1.6 for the BY condition, and to 1.5 for the achromatic conditions at 10 c/d. A similar trend of spatial frequency–dependent binocular summation was observed at subthreshold level[31] for the RG condition, with summation ratios of 1.78 (5 dB) and 1.58 (4 dB) at low and high spatial frequency (0.375 and 1.5 c/d). respectively. However, this trend was not observed for the Ach condition, in which the ratio was 1.41 (3 dB) for both spatial frequencies. Furthermore, several other studies also have explored this issue at detection level for Ach,[32] and both Ach and RG conditions[31,33,34] with a low spatial frequency (0.5 c/d).

These observations are also quantified by comparing the parameters of the sensitivity functions. Figure 5c shows the estimated values for the peak gain f_{max} averaged across the 20 subjects under the monocular ("M," left bar) and binocular ("B," right bar) presentations for the RG, BY, and Ach conditions. Results show that the estimated peak gain value for the binocular presentation is significantly higher than for the monocular one (Wilcoxon signed rank test, $\alpha = 0.05$) for the three contrast conditions, indicating a superior sensitivity

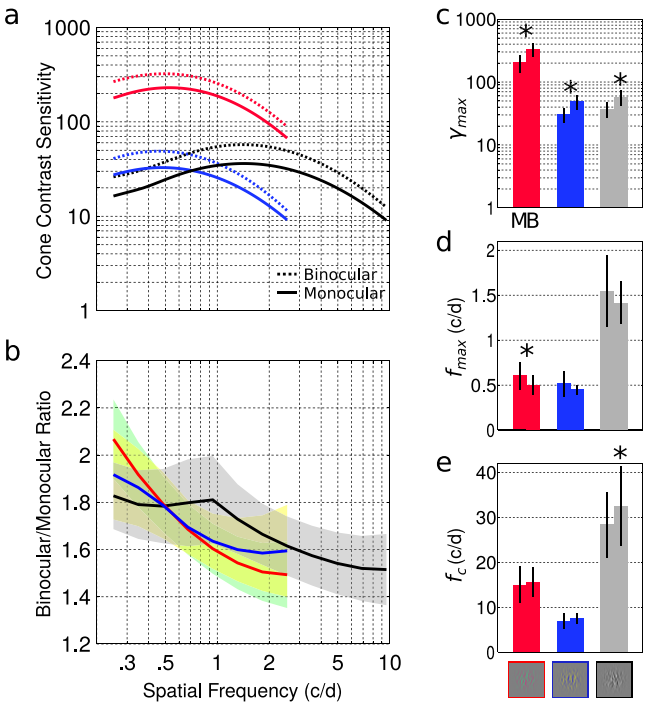

Figure 5. Binocular summation. (**a**) CCSFs for the monocular (*solid lines*) and binocular (*dotted lines*) presentations averaged across the 20 subjects are plotted for the Ach (*black*), RG (*red*), and BY (*blue*) conditions. (**b**) The averaged ratio of the binocular to the monocular sensitivity across spatial frequency is plotted for the Ach, RG, and BY conditions. The *shaded regions* represent ± SE. (**c–e**) The estimated values of the peak gain γ_{max} (**c**), peak spatial frequency f_{max} (**d**), and cutoff spatial frequency f_c (**e**) for the monocular ("M," *left bar*) and binocular ("B," *right bar*) presentations for the RG (*red*), BY (*blue*), and Ach (*gray*) conditions averaged across the subjects are plotted. *Error bars* are SD. The *asterisk* indicates that the estimated values obtained from the monocular and binocular presentations are significantly different (paired Wilcoxon signed rank test, $\alpha = 0.05$).

for the binocular presentation compared with the monocular one. No change is observed in the peak spatial frequency f_{max}, as shown in Figure 5d. However, a concomitant increase in the cutoff spatial frequency f_c is observed only for the achromatic condition, as shown in Figure 5e.

Discussion

We have determined the absolute CCSs for the three cardinal directions in the cone contrast space over a range of spatial frequencies for a healthy population, providing direct comparisons between achromatic and the two chromatic postreceptoral CCSs. This study provides a number of novel contributions: a normative data set for the achromatic and two chromatic CSFs using an abbreviated approach potentially suitable for clinical practice; a quantitative comparison of achromatic, RG chromatic, and BY chromatic sensitivity as a function of spatial frequency in a common cone contrast space; and a detailed comparison of achromatic, RG chromatic, and BY chromatic binocular summation as a function of spatial frequency.

Clinical practice is well served by a wide variety of well-established color vision tests that focus on defining the patterns of color vision losses within specified color spaces to characterize the different forms of congenital color vision deficiencies, including the pseudoisochromatic plates for inherited color vision deficiencies,[35] the Farnsworth-Munsell 100-hue test and D15 test,[36] the Lanthony desaturated D15,[37] the Mollon-Reffin minimal color test,[38] and the screen-based City University dynamic color vision test.[39] These tests are not specifically designed for quantifying any deficiencies in color vision associated with the postreceptoral processes and do not take into account any dependence on the spatial properties of the stimulus, both of which are more likely to be associated with acquired vision disorders. The more recent "cone contrast test"[18] is closer to our approach in that it uses a cone contrast metric and measures contrast detection thresholds; however, it tests sensitivity to letter stimuli (of fixed size) using contrasts that isolate the individual L, M, and S cone types, and so will target the diagnosis of cone-based color vision defects.

A *qCSF* Normative Data Set

We have used the *qCSF*[19,20] approach to characterize the monocular cone CSFs for the achromatic Ach, RG, and BY chromatic stimuli for 51 young adults to provide a normative dataset ($n = 51$) (Figs. 2, 3). To be able to compare these three sensitivities using a common cone contrast space has potential advantages clinically, because different postreceptoral mechanisms may be affected in different conditions. The inclusion of BY contrast sensitivities is important because in general retinal pathologies are known to selectively affect BY sensitivity, whereas optic nerve pathologies may affect RG sensitivity selectively, and cortical pathologies both RG and BY contrast sensitivity.[39–44] The current results, as shown in Figure 4, revealed a significant correlation between the RG and BY sensitivity, and this finding is surprising because the underlying mechanisms subserving the RG and BY cone contrast sensitivities are presumed to be independent at threshold,[12,13,45–48] although there is some support for a weak S-cone input to the RG chromatic mechanism.[13,48,49] This data set is for subjects of mean age 25.8 ± 7.2 SD and it would not be expected to apply across the age range. Age-dependent optical (e.g., yellowing of the lens, loss of lens transparency, pupillary miosis) as well as possibly neural changes would reduce not only the spatial resolution but also the peak sensitivity of these functions. There will be a need to extend this work to older subjects before this approach is of use in clinical populations.

Binocular Summation of Chromatic and Achromatic Contrast

Binocular summation is one of a number of different indexes to binocularity and has received attention recently as it has provided evidence that strabismic amblyopes,[50] previously thought not to have binocular function, do have a latent form of binocularity that can lead into a successful treatment.[51] Using a common cone contrast metric, we have revealed that binocular summation depends not only on stimulus chromaticity (i.e., RG, BY, and Ach) but also on stimulus spatial frequency (Fig. 5b). The current observation is the first to have measured the binocular summation ratio within a common cone contrast space over a wide spatial frequency range for the three different chromatic stimuli (RG, BY, and Ach) in a large sample of healthy observers. Many previous studies have explored binocular summation using only achromatic luminance contrast at detection threshold.[32,52–56] Some studies have investigated binocular summation using chromatic as well as achromatic stimuli at detection threshold[33,34] and at subthreshold levels[31] in small-scale laboratory studies. Their results are also consistent with the notion that binocular summation depends on the spatial frequency, varying from approximately 1.78 to 2.0 at low spatial frequencies (0.375–0.5

c/d) to approximately 1.41 at high spatial frequencies (1.5 c/d).[31–34] It is apparent from Figure 5c that binocular viewing not only results in a vertical translation of the sensitivity function (gain), but also a change in the bandwidth of the function. We believe that these summation results reflect neural processing rather than, for example, optical factors such as accommodation being more accurate under binocular as opposed to monocular viewing conditions. For low-contrast targets such as the ones presented here, accommodation accuracy does not depend on target spatial frequency for the range that we have investigated here,[57] so it is unlikely that the better summation at lower spatial frequencies can be explained in terms of the accommodative response.

Acknowledgments

The authors thank all subjects for participating in the study.

Supported in part by Canadian Institutes of Health Research Grants 10818 (RFH) and 10819, and Natural Science and Engineering Research Council Grant RGPIN 183625-05 (KTM).

Disclosure: **Y.J. Kim**, None; **A. Reynaud**, None; **R.F. Hess**, None; **K.T. Mullen**, None

References

1. Gstalder RJ, Green DG. Laser interferometric acuity in amblyopia. *J Pediatr Ophthalmol*. 1971;8:251–256.
2. Bodis-Wollner I. Visual acuity and contrast sensitivity in patients with cerebral lesions. *Science*. 1972;178:769–771.
3. Hess RF, Howell ER. The threshold contrast sensitivity function in strabismic amblyopia: evidence for a two type classification. *Vision Res*. 1977;17:1049–1055.
4. Levi DM, Harwerth RS. Spatio-temporal interactions in anisometropic and strabismic amblyopia. *Invest Ophthalmol Vis Sci*. 1977;16:90–95.
5. Atkin A, Bodis-Wollner I, Wolkstein M, Moss A, Podos SM. Abnormalities of central contrast sensitivity in glaucoma. *Am J Ophthalmol*. 1979;88:205–211.
6. Hyvärinen L, Laurinen P, Rovamo J. Contrast sensitivity in evaluation of visual impairment due to macular degeneration and optic nerve lesions. *Acta Ophthalmol (Copenh)*. 1983;61:161–170.
7. Hess RF, Plant GT. *Recent Advances in Optic Neuritis*. Cambridge: Cambridge University Press; 1986.
8. Dacey DM, Crook JD, Packer O. Distinct synaptic mechanisms create parallel S-ON and S-OFF color opponent pathways in the primate retina. *Vis Neurosci*. 2013;31:139–151.
9. Lee BB, Martin PR, Grünert U. Retinal connectivity and primate vision. *Prog Retin Eye Res*. 2010;29:622–639.
10. Crook JD, Davenport CM, Peterson BB, Packer OS, Detwiler PB, Dacey DM. Parellel ON and OFF cone bipolar inputs establish spatially coextensive receptive field structure of blue-yellow ganglion cells in primate retina. *J Neurosci*. 2009;29:8372–8387.
11. Hendry SH, Reid RC. The koniocellular pathway in primate vision. *Annu Rev Neurosci*. 2000;23:127–153.
12. Cole GR, Hine T, McIlhagga W. Detection mechanisms in L-, M-, and S-cone contrast space. *J Opt Soc Am A*. 1993;10:38–51.
13. Sankeralli MJ, Mullen KT. Estimation of the L-, M- and S-cone weights of the post-receptoral detection mechanisms. *J Opt Soc Am A*. 1996;13:906–915.
14. Cole GR, Hine T. Computation of cone contrasts for color vision research. *Behav Res Methods Instrum Comput*. 1992;24:22–27.
15. Kelly DH. Spatiotemporal variation of chromatic and achromatic contrast thresholds. *J Opt Soc Am A*. 1983;73:742–750.
16. Mullen KT. The contrast sensitivity of human colour vision to red-green and blue-yellow chromatic gratings. *J Physiol (Lond)*. 1985;359:381–400.
17. Mullen KT, Thompson B, Hess RF. Responses of the human visual cortex and LGN to achromatic and chromatic temporal modulations: an fMRI study. *J Vis*. 2010;10(13):13.
18. Rabin J, Gooch J, Ivan D. Rapid quantification of colorvision: the cone contrast test. *Invest Ophthalmol Vis Sci*. 2011;52:816–820.
19. Lesmes LA, Lu Z-L, Baek J, Albright TD. Bayesian adaptive estimation of the contrast sensitivity function: the quick CSF method. *J Vis*. 2010;10(3):17.
20. Hou F, Huang C–B, Lesmes L, et al. qCSF in clinical application: efficient characterization and classification of contrast sensitivity functions in amblyopia. *Invest Ophthalmol Vis Sci*. 2010;51:5365–5377.
21. Borish I. Photometry and stereopsis. In: Benjamin WJ, ed. *Borish's Clinical Refraction*. 2nd ed. London: Elsevier Health Sciences; 2006:899–962.
22. Smith VC, Pokorny J. Spectral sensitivity of the foveal cone photopigments between 400 and 500 nm. *Vision Res*. 1975;15:161–171.
23. Brainard D. Cone contrast and opponent modulation color spaces. In: Kaiser PK, Boynton RM, eds. *Human Color Vision*. 2nd ed. Washington, DC: Optical Society of America; 1996:563–579.
24. Ahumada AJ, Peterson HA. Luminance-model-based DCT quantization for color image compression. In: Rogowitz BE, ed. *Human Vision, Visual Processing, and Digital Display III*. Proc SPIE. 1992;1666:365–374.
25. Watson AB, Ahumada AJ. A standard model for foveal detection of spatial contrast. *J Vis*. 2005;5(9):6.
26. Robson JG. Spatial and temporal contrast-sensitivity functions of the visual system. *J Opt Soc Am A*. 1966;56:1141–1142.
27. Wuerger SM, Watson AB, Ahumada AJ. Towards a spatio-chromatic standard observer for detection. *Proc SPIE Int Soc Opt Eng*. 2002;4662:159–172.
28. Stromeyer CF III, Cole GR, Kronauer RE. Second-site adaptation in the red-green chromatic pathways. *Vision Res*. 1985;25:219–237.
29. Chaparro A, Stromeyer CF III, Huang EP, Kronauer RE, Eskew RT Jr. Colour is what the eye sees best. *Nature*. 1993;361:348–350.
30. William D, Sekiguchi N, Brainard D. Color, contrast sensitivity, and the cone mosaic. *Proc Natl Acad Sci U S A*. 1993;90:9770–9777.
31. Gheiratmand M, Cherniawsky AS, Mullen KT. Orientation tuning of binocular summation: a comparison of colour to achromatic contrast. *Sci Rep*. 2016;6:1–9.
32. Legge GE. Binocular contrast summation–I. Detection and discrimination. *Vision Res*. 1984;24:373–383.
33. Simmons DR, Kingdom FA. On the binocular summation of chromatic contrast. *Vision Res*. 1998;38:1063–1071.
34. Simmons DR. The binocular combination of chromatic contrast. *Perception*. 2005;34:1035–1042.
35. Ishihara S. *Tests for Color-blindness*. Tokyo, Handaya: Hongo Harukicho; 1917.
36. Farnsworth D. The Farnsworth-Munsell 100-hue and dichotomous tests for color vision. *J Opt Soc Am*. 1943;33:568–578.
37. Lanthony P, Dubios-Poulsen A. Le Farnsworth-15 désaturé. *Bull Soc Ophtalmol Fr*. 1978;73:861–866.
38. Reffin JP, Astell S, Mollon JD. Trials of a computer-controlled colour vision test that preserves the advantages of psedoisochromatic plates. In: Drum B, Moreland JD, Serra A, eds. *Colour Vision Deficiencies X. Documenta Ophthalmologica*

Proceedings Series, Volume 53. Dordrecht, The Netherlands: Kluwer; 1991:69–76.

39. Barbur JL, Harlow AJ, Plant GT. Insights into the different exploits of colour in the visual cortex. *Proc R Soc Lond B Biol Sci*. 1994;258:327–334.
40. Köllner H. *Die Störungen des Farbensinners. Ihre klinische Bedeutung und ihre Diagnose*. Berlin: Karger; 1912.
41. Pacheco-Cutillas M, Edgar DF. Acquired colour vision defects in glaucoma—their detection and clinical significance. *Br J Ophthalmol*. 1999;83:1396–1402.
42. Katz B. The dyschromatopsia of optic neuritis: a descriptive analysis of data from the optic neuritis treatment trial. *Trans Am Ophthalmol Soc*. 1995;93:685–708.
43. Al-Hashmi AM, Kramer DJ, Mullen KT. Human vision with a lesion of the parvocellular pathway: an optic neuritis model for selective contrast sensitivity deficits with severe loss of midget ganglion cell function. *Exp Brain Res*. 2011;215:293–305.
44. Hess RF, Thompson B, Gole G, Mullen KT. The amblyopic deficit and its relationship to geniculo-cortical processing streams. *J Neurophysiol*. 2010;104:475–483.
45. Noorlander C, Heuts MJG, Koenderink JJ. Sensitivity to spatiotemporal combined luminance and chromaticity contrast. *J Opt Soc Am A*. 1981;71:453–459.
46. Dobkins KR, Gunter KL, Peterzell DH. What covariance mechanisms underlie green/red equiluminance, luminance contrast sensitivity and chromatic (green/red) contrast sensitivity? *Vision Res*. 2000;40:613–628.
47. Peterzell DH, Teller DY. Spatial frequency tuned covariance channels for red-green and luminance-modulated gratings: psychophysical data from human adults. *Vision Res*. 2000;40:417–430.
48. Gunther KL, Dobkins KR. Independence of mechanisms tuned along cardinal and non-cardinal axes of color space: evidence from factor analysis. *Vision Res*. 2003;43:683–696.
49. Costa MF, Goulart RK, Barboni MT, Ventura DF. Reduced discrimination in the tritanopic confusion line for congenital color deficiency adults. *Front Psychol*. 2016;7:429.
50. Baker DH, Meese TS, Mansouri B, Hess RF. Binocular summation of contrast remains intact in strabismic amblyopia. *Invest Ophthalmol Vis Sci*. 2007;48:5332–5338.
51. Li J, Thompson B, Deng D, Chan LYL, Yu M, Hess RF. Dichoptic training enables the adult amblyopic brain to learn. *Curr Biol*. 2013;23:308–309.
52. Campbell FW, Green DG. Monocular versus binocular visual acuity. *Nature*. 1965;208:191–192.
53. Blake R, Fox R. The psychophysical inquiry into binocular summation. *Percept Psychophys*. 1973;14:161–185.
54. Blake R, Sloane M, Fox R. Further developments in binocular summation. *Percept Psychophys*. 1981;30:266–276.
55. Legge GE. Binocular contrast summation–II. Quadratic summation. *Vision Res*. 1984;24:385–394.
56. Meese TS, Georgeson MA, Baker DH. Binocular contrast vision at and above threshold. *J Vis*. 2006;6(11):7.
57. Xu J, Zheng Z, Drobe B, Jiang J, Chen H. The effect of spatial frequency on the accommodation responses of myopes and emmetropes under various detection demands. *Vision Res*. 2015;115:1–7.

Appendix

Control Conditions (With the Method of Constant Stimuli)

In a control experiment, the chromatic sensitivity functions measured with the *qCSF* in the main experiments (Figs. 2, 3) are compared with the sensitivity functions measured with the Method of Constant Stimuli (MCS) for the RG and BY chromatic conditions for each spatial frequency: 0.24, 0.33, 0.46, 0.64, 0.89, 1.23, 1.72, and 2.39 c/d for six subjects. The order in which participants performed the different spatial frequency conditions is randomized. The contrast levels used are 0.0013, 0.0018, 0.0025, 0.0035, 0.005, 0.0071, 0.01, 0.014, 0.02, 0.028, and 0.04 for the RG condition, and 0.013, 0.018, 0.025, 0.035, 0.05, 0.071, 0.1, 0.14, 0.2, 0.28, and 0.4 for the BY condition. There are 20 repetitions per each contrast. Each measurement takes approximately 10 minutes. The detection thresholds are determined by fitting a Weibull function of the log-levels to the psychometric datasets (Equation 4, maximum likelihood estimation method).

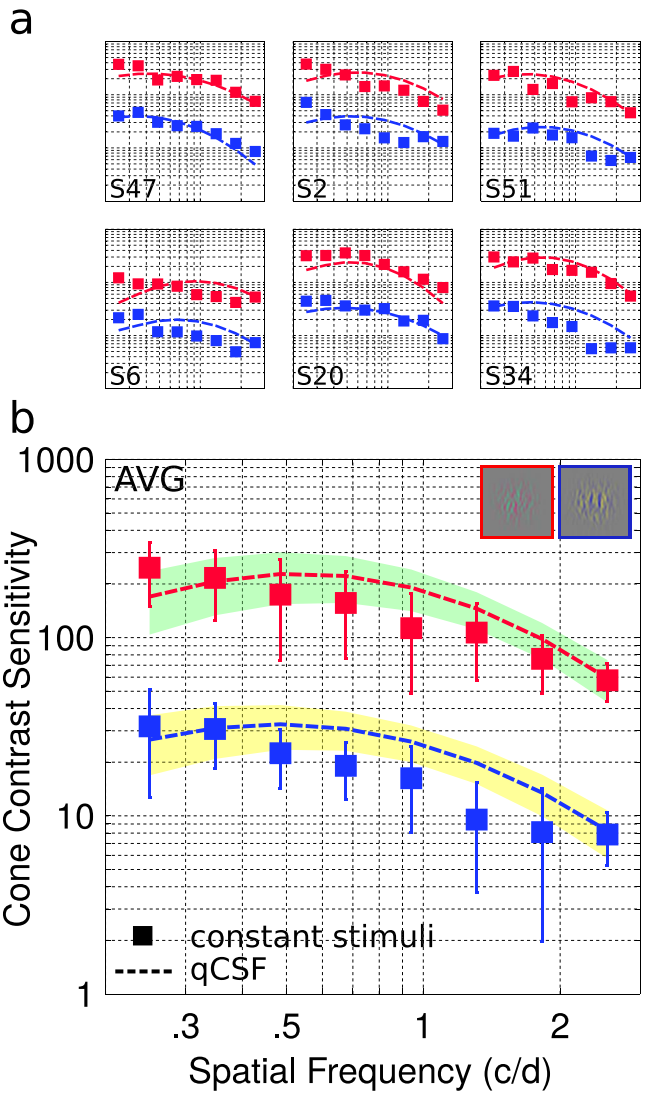

Figure A1. Methods comparison. (**a**) The different panels represent an individual's CCSFs for the RG (*red*) and BY (*blue*) conditions measured using the MCS (*squares*), and the *qCSF* method (*dotted lines*, Fig. 3). (**b**) CCS functions averaged across the six subjects for the RG and BY conditions are shown in (**a**). *Error bars* and *shaded regions* represent ± SD.

$$F_W(x;\alpha,\beta) = 0.5 + 0.5 \cdot \left(1 - e^{-\left(\frac{x}{\alpha}\right)^{\beta}}\right) \quad (4)$$

where x indicates the log-levels, α the log-threshold, and β the slope of the psychometric function.

The CCS functions measured using the *qCSF* and the MCS for the six subjects are plotted together in the appendix figure. Data obtained from different methods are similar to each other, as shown in the Figure A1a (individual data) and Figure A1b (average data). Note that the *qCSF* method shows a tendency to underestimate the sensitivity at low spatial frequency and overestimate it at middle spatial frequency, possibly resulting in an overestimation of the peak spatial frequency f_c.

Investigative Ophthalmology & Visual Science